Electronic Supplementary Material (ESI) for ChemComm.

Supporting Information

Heterogeneous Mesoporous Manganese Oxide Catalyst for Aerobic and Additive-Free Oxidative Aromatization of N-Heterocycles

Kankana Mullick, Sourav Biswas, Alfredo M. Angeles-Boza, and Steven L. Suib**

Preparation of meso MnO_x

The catalyst was synthesized following the procedure described by Poyraz *et al*.[1] In a typical synthesis 0.02 mol of manganese nitrate tetrahydrate (Mn $(NO_3)_2 \cdot 4H_2O$, 0.02 mol) and 0.134 mol of 1-butanol were added into a 120 mL beaker. To this solution 0.0034 mol of poly(ethylene glycol)-block-poly(propylene glycol)-block-poly(ethylene glycol) (Pluoronic P123, $PEO_{20}PPO_{70}PEO_{20}$, molar mass 5750 g mol^{-1}) and 0.032 mol of concentrated nitric acid (HNO_3) were added and stirred at room temperature until the solution became clear (light pink). The resulting clear solution was then kept in an oven at 120°C for 3 h. After reaction, the black product was washed with excess ethanol, centrifuged, and dried in a vacuum oven overnight. At the end, the dried black powders were subjected to a heating cycle. First they were heated at 150°C for 12 h and cooled down to room temperature followed by heated to 250°C for 4 h.

Reaction procedure of oxidative aromatization

In a typical reaction, a mixture of 1,2,3,4-tetrahydroquinoline (0.25 mmol), meso MnO_x (25 mg) and DMF (5 mL) was added in a 25 mL round bottom flask (two-necked flask was used for time dependent study) equipped with a condenser. The reaction mixture was heated to reflux under vigorous stirring (700 rpm) for the required time under an air balloon. After reaction, the mixture was cooled and the catalyst was removed by filtration. The product analysis was done using GC-MS (gas chromatography-mass spectrometry). The conversion was determined based on the concentration of substrate. Most reactions were repeated twice and the average values were used. The products were isolated by filtering off the catalyst followed by evaporation of solvent. For isolation, the reactions have been performed in acetonitrile (at 80°C) for easy solvent evaporation.

Analysis of reaction products

The GC-MS analyses were performed by a 7820A GC system connected with a mass detector of 5975 series MSD from Agilent Technologies and a nonpolar cross-linked methyl siloxane column with dimensions of 12 in × 0.200 mm × 0.33 μm was used. The ^{1}H and ^{13}C NMR spectra were recorded on a Bruker AVANCE III- 400 MHz spectrometer. ^{1}H NMR spectra were collected at 400 MHz with chemical shift referenced to the residual peak in $CDCl_3$ (δ: H 7.26 ppm). ^{13}C NMR spectra were collected at 100 MHz and referenced to residual peak in $CDCl_3$ (δ: C 77.0 ppm). Multiplicities are written as s (singlet), d (doublet), t (triplet), and m (multiplet).

Catalyst Characterizations

The powder X-Ray diffraction (PXRD) data were collected by a Rigaku Ultima IV diffractometer (Cu Kα radiation, λ=1.5406 Å) with an operating voltage of 40 kV and a current of 44 mA. The PXRD patterns were collected over a 2θ range of 5–75° with a continuous scan rate of 1.0° min^{-1}. The Nitrogen adsorption desorption experiments were performed with a Quantachrome Autosorb-1-1C automated adsorption system. The samples were treated at 150°C for 6 h under helium prior to measurement. X-ray photoelectron spectroscopy (XPS) was done on a PHI model 590 spectrometer with multiprobes (ΦPhysical Electronics Industries Inc.), using Al-K radiation (λ= 1486.6 eV) as the radiation source and was fitted using CasaXPS software (version 2.3.12). The powder samples were pressed on carbon tape mounted on adhesive copper tape stuck to a sample stage placed in the analysis chamber. For correction of surface charging, the C 1s photoelectron line at 284.6 eV was taken as a reference. A mixture of Gaussian (70%) and Lorentzian (30%) functions was used for the least-squares curve fitting procedure.

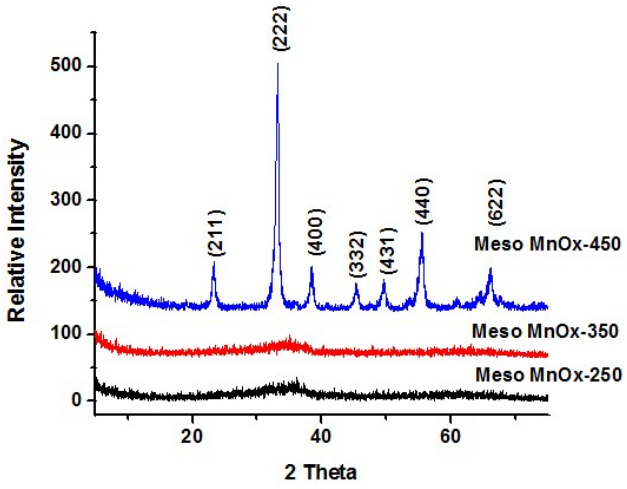

Figure S1. Powder X-ray diffraction of meso MnOx at different calcination temperatures. The diffraction patterns at 450°C calcination can be indexed to Mn_2O_3 phase, whereas calcination temperatures at 250°C and 350°C displayed an amorphous nature.

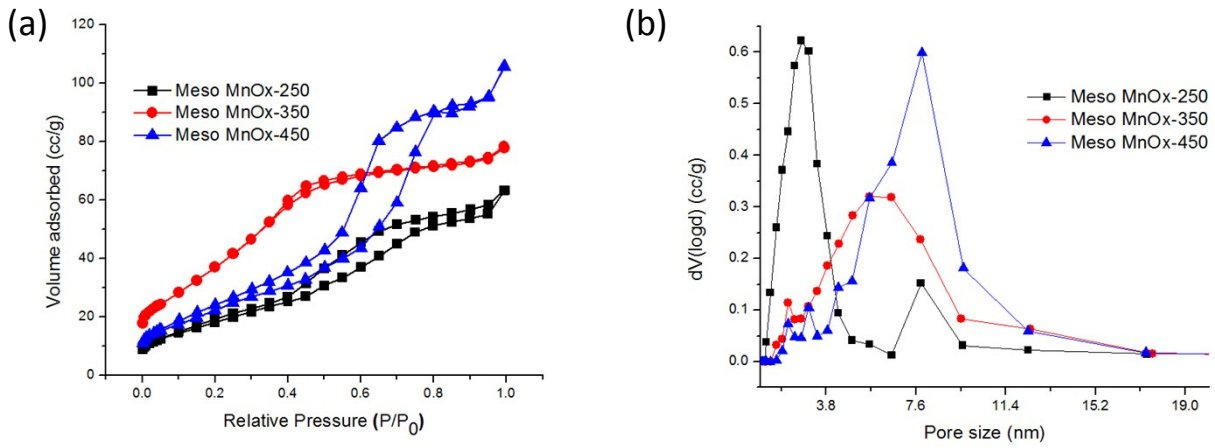

Figure S2. (a) Nitrogen adsorption isotherms of meso MnOx at different calcination temperatures. A type IV adsorption isotherm followed by a type I hysteresis loop were observed for all the materials, which confirmed the mesoporous structure and (b) corresponding BJH adsorption pore size distribution

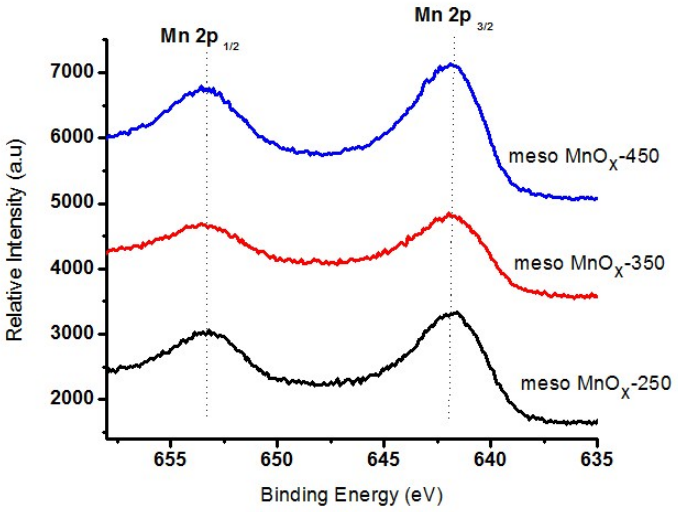

Figure S3. XPS of Mn2p of meso MnO_x at different calcination temperatures. The $Mn2p_{3/2}$ binding energy of (641.5±0.2) eV indicates Mn^{3+} oxidation state at all calcination temperatures

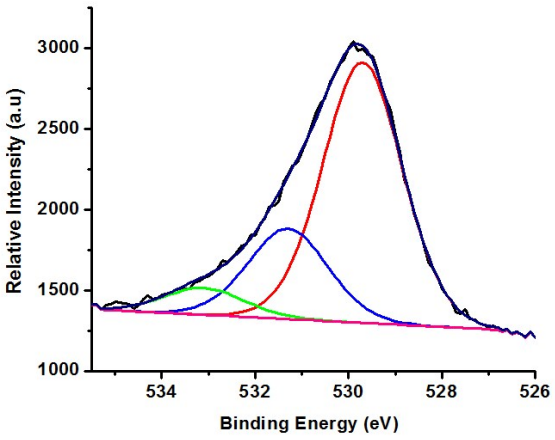

Figure S4. XPS analysis deconvoluted O1s spectra of meso $MnO_{x\text{-}250}$. O_s (red line): Structural or lattice oxygen, O_{ads} (blue line): Adsorbed oxygen on the surface, O_{mw} (green line): Adsorbed water and hydroxyl group.

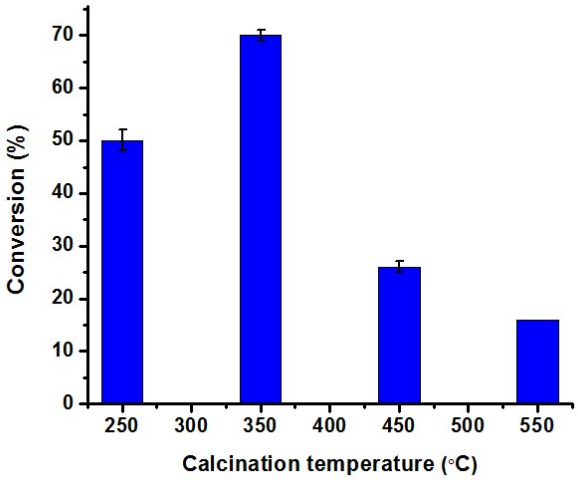

Figure S5. Effect of calcination temperature in the performance of meso MnO_x. Reaction condition: 1,2,3,4-tetrahydroquinoline (0.25 mmol), meso MnO_x (25 mg), DMF (5 mL), 130°C, air balloon, 5 h.

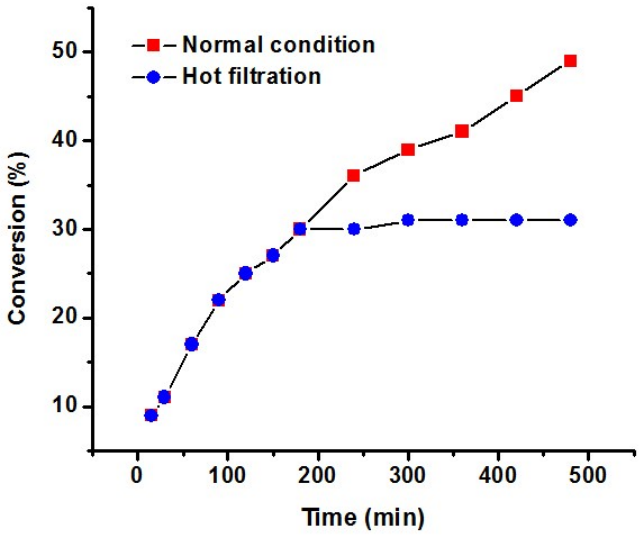

Figure S6. Hot filtration test. Reaction condition: 1,2,3,4-tetrahydroquinoline (0.25 mmol), meso MnO_x (25 mg), DMF (5 mL), 130°C, air balloon. Catalyst was removed at 30% conversion (at 3 h).

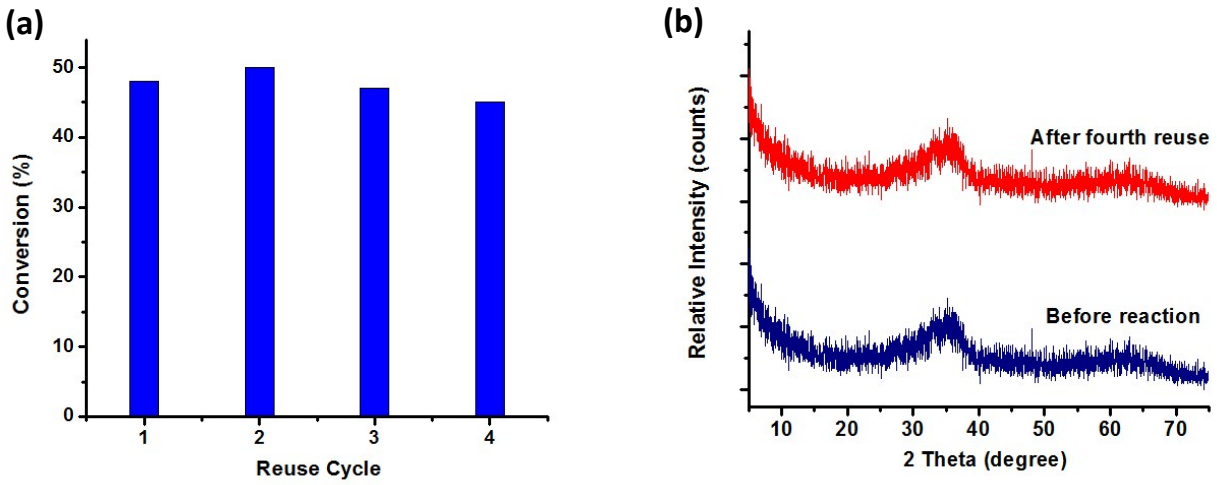

Figure S7. (a) Reusability test. Reaction condition: 1,2,3,4-tetrahydroquinoline (0.25 mmol), meso MnO_x (25 mg), DMF (5 mL), 130°C, air balloon, 5 h. (b) PXRD before and after fourth reuse.

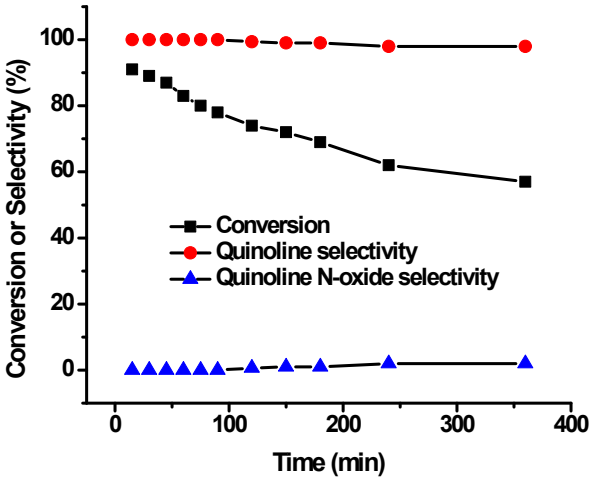

Figure S8. Time dependent study. Reaction condition: 1,2,3,4-tetrahydroquinoline (0.25 mmol), meso MnO_x (25 mg), DMF (5 mL), 130°C, air balloon.

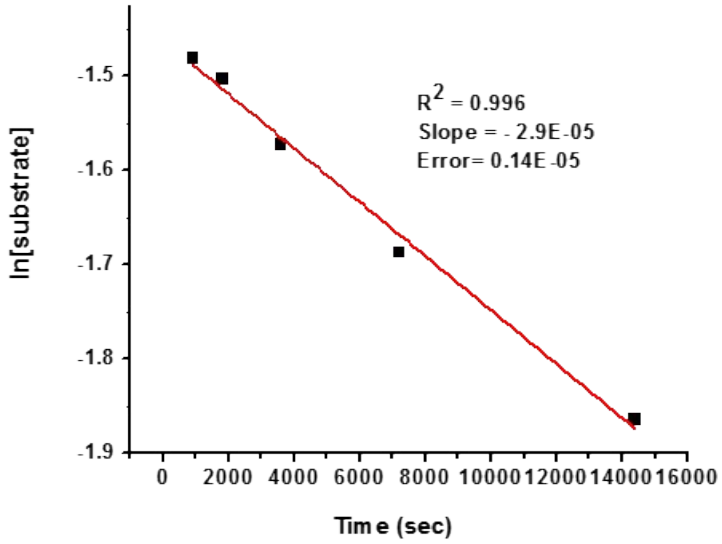

Figure S9. Kinetic study. Reaction condition: 1,2,3,4-tetrahydroquinoline (0.25 mmol), meso MnO_x (25 mg), DMF (5 mL), 130°C, air balloon. The reaction depreciated a first order rate with respect to substrate having a rate constant of $3\times10^{-5}\pm0.1\times10^{-5}s^{-1}$.

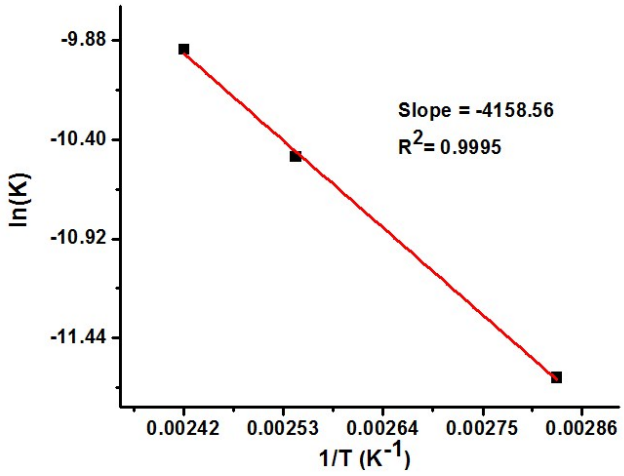

Figure S10. Arrhenius plot for the oxidation of 1,2,3,4-tetrahydroquinoline by meso MnO_x. The apparent activation energy was estimated as 8.3±0.2 Kcal mol^{-1}. Reaction condition: 1,2,3,4-tetrahydroquinoline (0.25 mmol), meso MnO_x (25 mg), DMF (5 mL), 5 h, air balloon. K: rate constant.

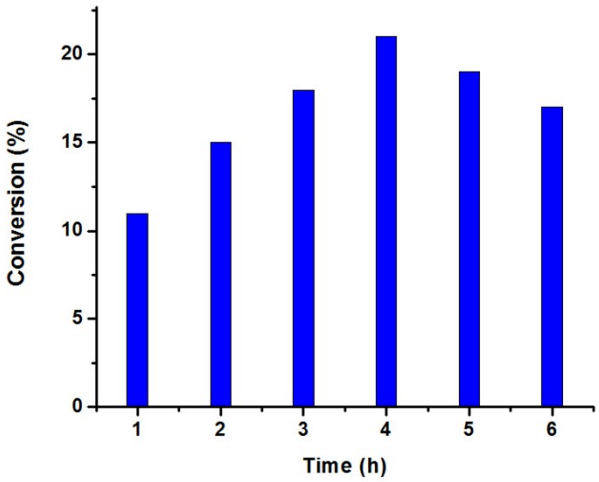

Figure S11. Kinetic study under nitrogen atmosphere. Reaction condition: 1,2,3,4-tetrahydroquinoline (0.25 mmol), meso MnO_x (25 mg), DMF (5 mL), 130°C, nitrogen balloon.

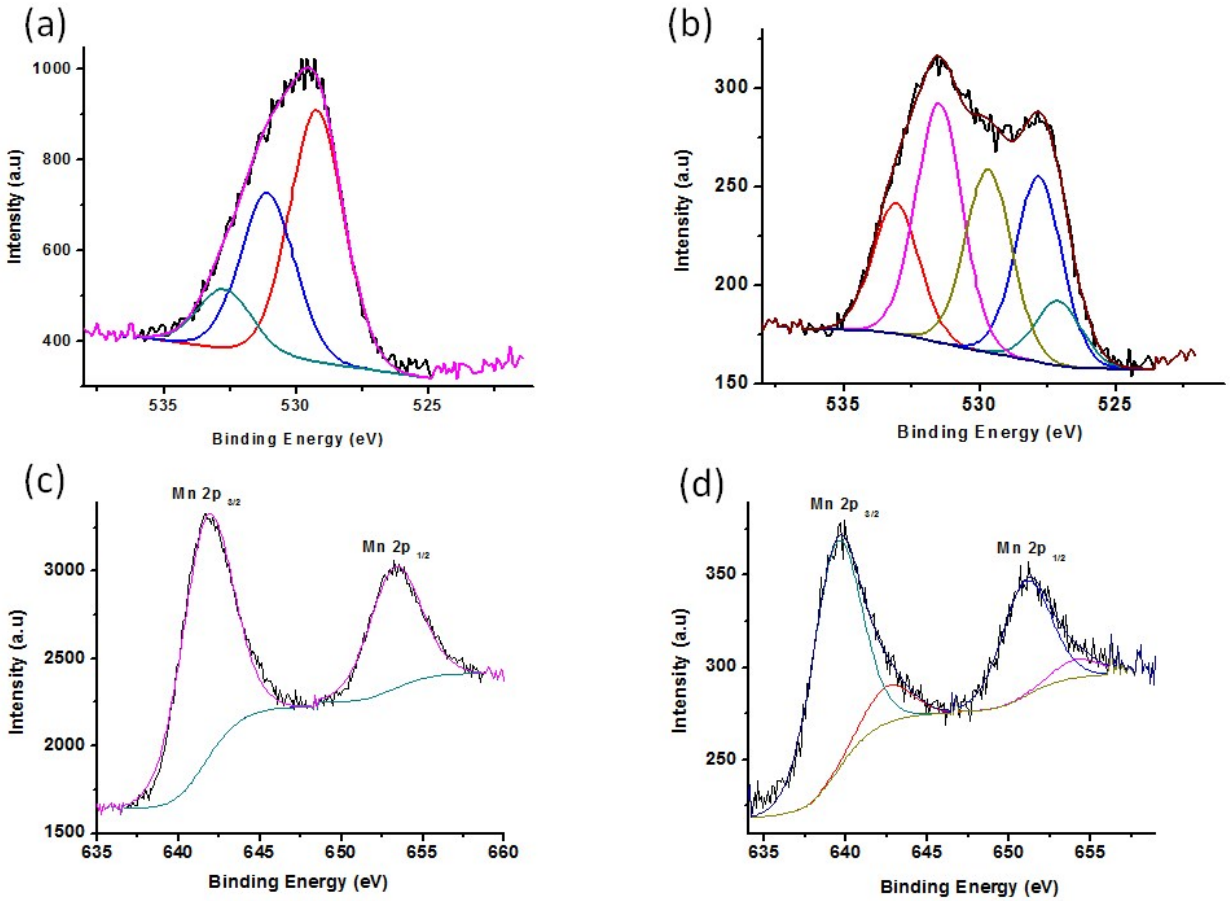

Figure S12. XPS of meso MnOx. O 1s (a) before reaction and (b) after reaction under nitrogen. And Mn 2p (c) before reaction and (d) after reaction under nitrogen.

Table S1. Effect of solvents in aromatization of 1,2,3,4-tetrahydroquinoline

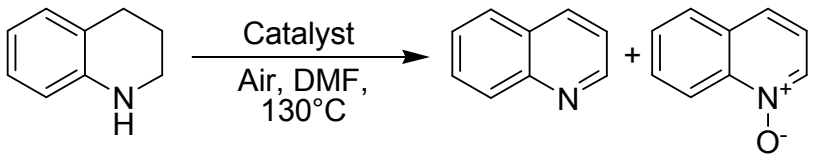

Entry	Solvent	Temperature (°C)	Conversion[b] (%)	Selectivity[b] (%)
1	DMF	130	50	>99
2	Acetonitrile	80	23	>99
3	Dioxane	100	28	>99
4	Toluene	110	15	>99
5	Hexane	60	14	>99

[a] Reaction conditions: 1,2,3,4-tetrahydroquinoline (0.25 mmol), meso MnO_x (25 mg), DMF (5 mL), 130°C, air balloon, 5 h. [b] Conversions and selectivity were determined by GC-MS based on concentration of 1,2,3,4-tetrahydroquinoline.

Table S2. Physicochemical properties of meso MnO_x at different calcination temperatures

Catalyst	Structure	Surface Area S_{BET} (m^2g^{-1})	BJH ads. pore size (nm)	Pore volume (cc g^{-1})
Meso MnO_x-250	Amorphous	182	2.8	0.21
Meso MnO_x-350	Amorphous	226	5.5	0.24
Meso MnO_x-450	Mn_2O_3	150	7.8	0.26

Table S3. Effect of oxidants and additives in aromatization of 1,2,3,4-tetrahydroquinoline

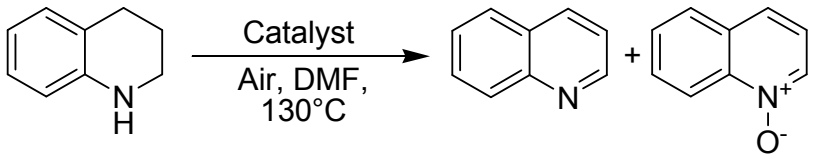

Entry	Oxidant	Additives	Conversion[b] (%)	Selectivity[b] (%)
1	Air	none	50	>99
2	O_2	none	49	83
3[c]	Air	none	25	>99
4[c]	O_2 (10 bar)	none	44	>99

[a] Reaction conditions: 1,2,3,4-tetrahydroquinoline (0.25 mmol), meso MnO_x (25 mg), DMF (5 mL), 130°C, air balloon, 5 h. [b] Conversions and selectivity were determined by GC-MS based on concentration of 1,2,3,4-tetrahydroquinoline. [c] 10 mg catalyst was used.

Table S4 Summary of XPS results

Meso MnOx	Mn (eV)				O_s		O_{ads}		O_{mw}	
	$2p_{3/2}$		$2p_{1/2}$		BE (eV)	%Area	BE (eV)	%Area	BE (eV)	%Area
Before reaction	641.7	-	652.4	-	529.2	62.6	530.9	27.3	532.8	9.9
Reaction under N_2	639.4	642.5	651.0	654.0	529.6	22.8	531.4	29.7	533.0	16.26

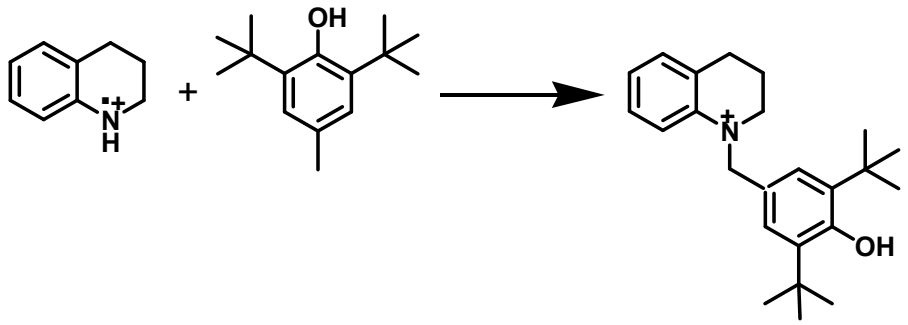

Scheme S1. Intermediate **I** Trapping: Reaction procedure: 1,2,3,4-tetrahydroquinoline (0.25 mmol) radical inhibitor (2.5 mmol), meso MnO_x (25 mg), DMF (5 mL), 130°C, air balloon, 5 h. The adduct was identified by GC-MS (molar mass 351).

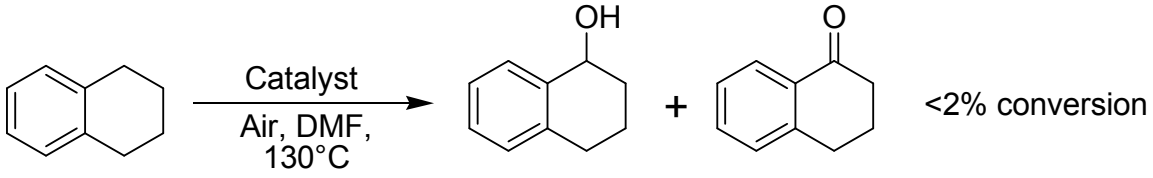

Scheme S2. Reaction with 1,2,3,4-tetrahydronaphlthalene. Reaction procedure: 1,2,3,4-tetrahydronaphlthalene (0.25 mmol) meso MnO_x (25 mg), DMF (5 mL), 130°C, air balloon, 5 h.

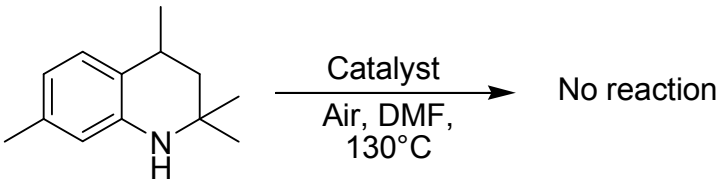

Scheme S3. Reaction with a 1,2,3,4-tetrahydroquinoline derivatives having double substitution at alpha position. Reaction procedure: 1,2,3,4-Tetrahydro-2,2,4,7-tetramethylquinoline (0.25 mmol) meso MnO_x (25 mg), DMF (5 mL), 130°C, air balloon, 5 h.

Characterization of typical products

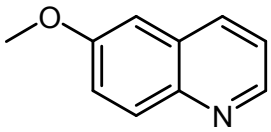

6-methoxyquinoline

Appearance: Yellow oil

^{1}H NMR (400 MHz, Chloroform-*d*) δ 8.76 (dd, *J* = 4.2, 1.5 Hz, 1H), 8.03 (dd, *J* = 19.4, 8.7 Hz, 2H), 7.36 (dt, *J* = 8.2, 3.3 Hz, 2H), 7.06 (d, *J* = 2.8 Hz, 1H), 3.92 (s, 3H).

^{13}C NMR (101 MHz, Chloroform-*d*): δ 158.02, 147.77, 144.21, 135.35, 130.57, 129.58, 122.71, 121.59, 105.34, 55.70.

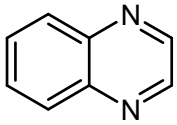

Quinoxaline

Appearance: Yellow oil

^{1}H NMR (400 MHz, Chloroform-d) δ 8.84 (s, 1H), 8.11 (dd, J = 6.4, 3.5 Hz, 1H), 7.78 (dd, J = 6.4, 3.4 Hz, 1H).

^{13}C NMR (101 MHz, Chloroform-*d*) δ 145.21, 130.32, 129.75.

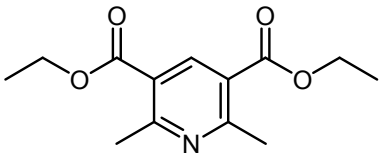

Diethyl 2,6-dimethylpyridine-3,5-dicarboxylate

Appearance: White powder

^{1}H NMR (400 MHz, Chloroform-*d*) δ 8.59 (s, *J* = 2.4Hz, 1H), 4.32 (m, *J* = 2.4Hz, 4H), 2.76 (d, *J* = 2.5 Hz, 6H), 1.34 (td, *J* = 2.5 Hz, 6H).

^{13}C NMR (101 MHz, Chloroform-*d*) δ 160.06, 162.35, 141.01, 123.19, 61.51, 25.09, 14.41.

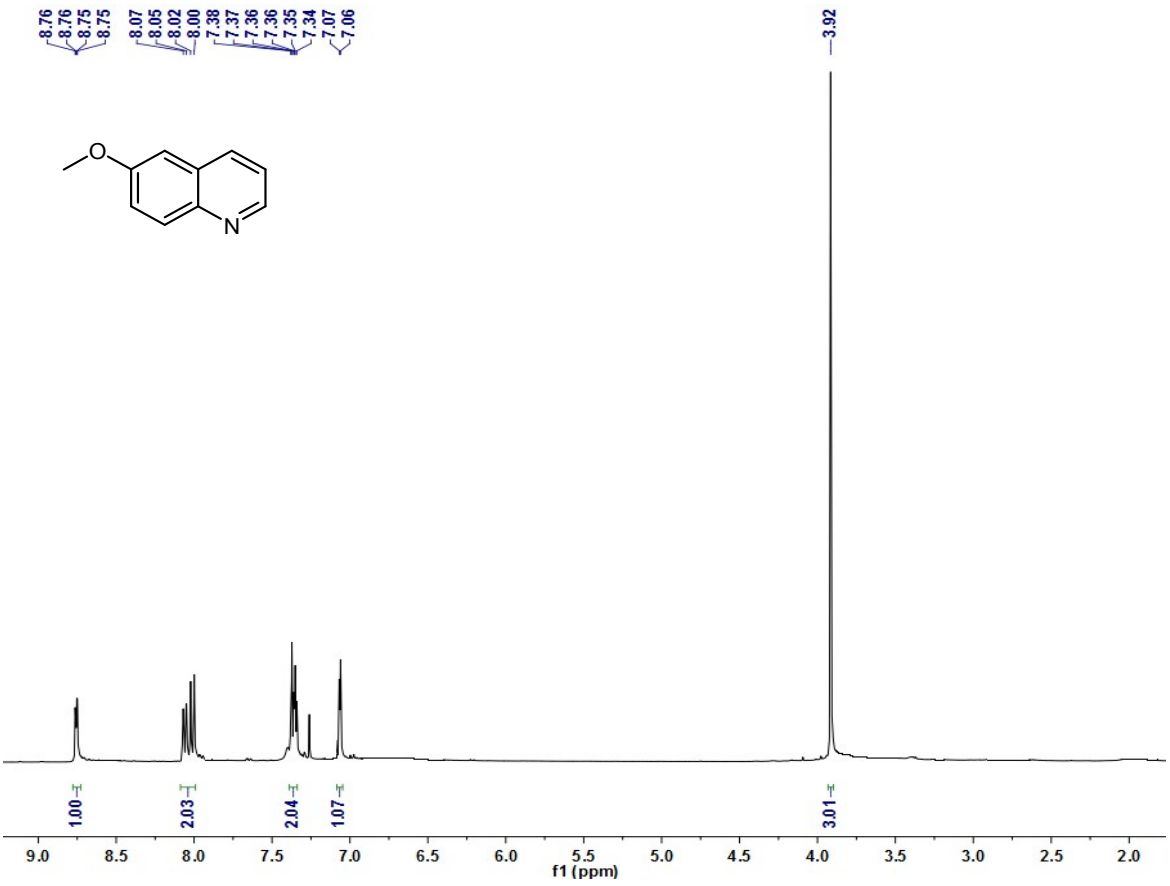
8.76
8.76
8.75
8.75
8.07
8.05
8.02
8.00
7.38
7.37
7.36
7.36
7.35
7.34
7.07
7.06
3.92
O
N
1.00
2.03
2.04
1.07
3.01
9.0
8.5
8.0
7.5
7.0
6.5
6.0
5.5
5.0
4.5
4.0
3.5
3.0
2.5
2.0
f1 (ppm)

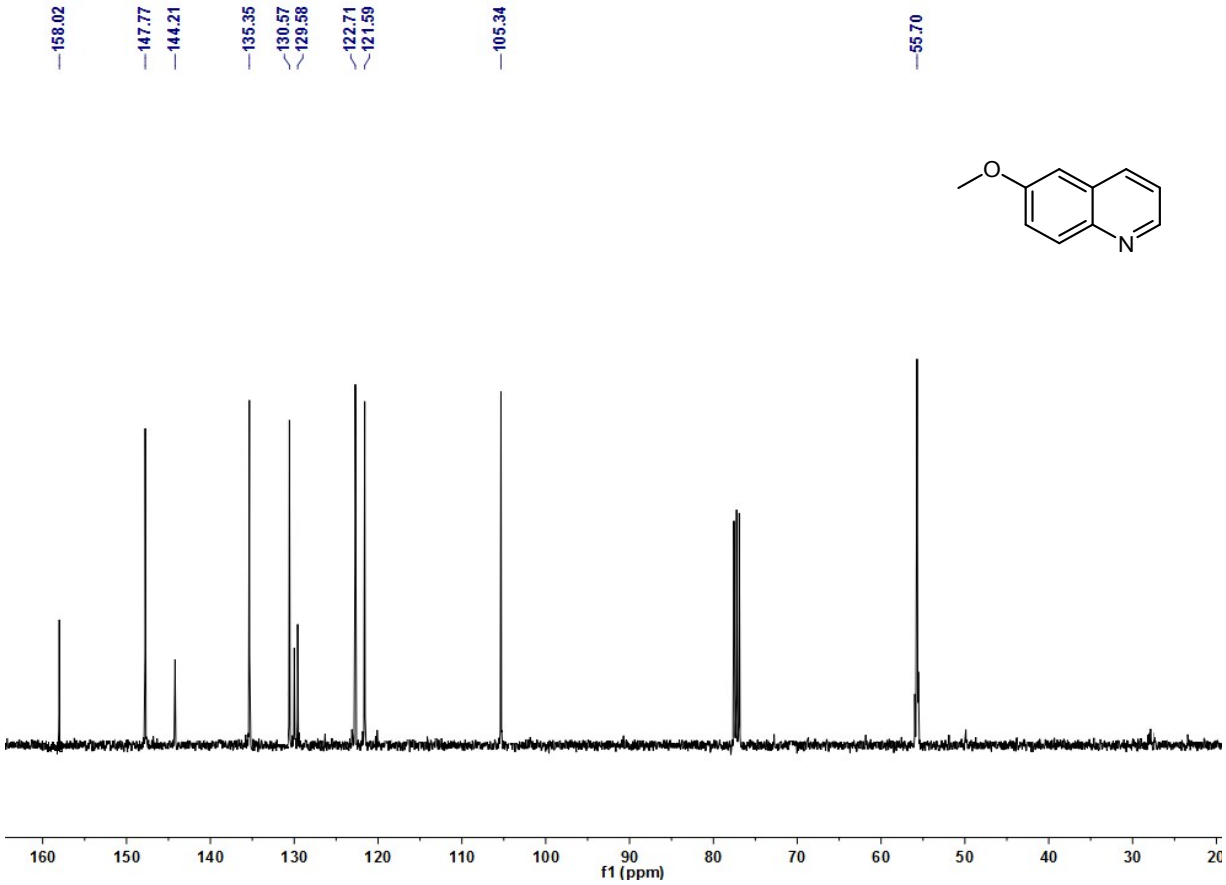
158.02
147.77
144.21
135.35
130.57
129.58
122.71
121.59
105.34
55.70
O
N
160
150
140
130
120
110
100
90
80
70
60
50
40
30
f1 (ppm)

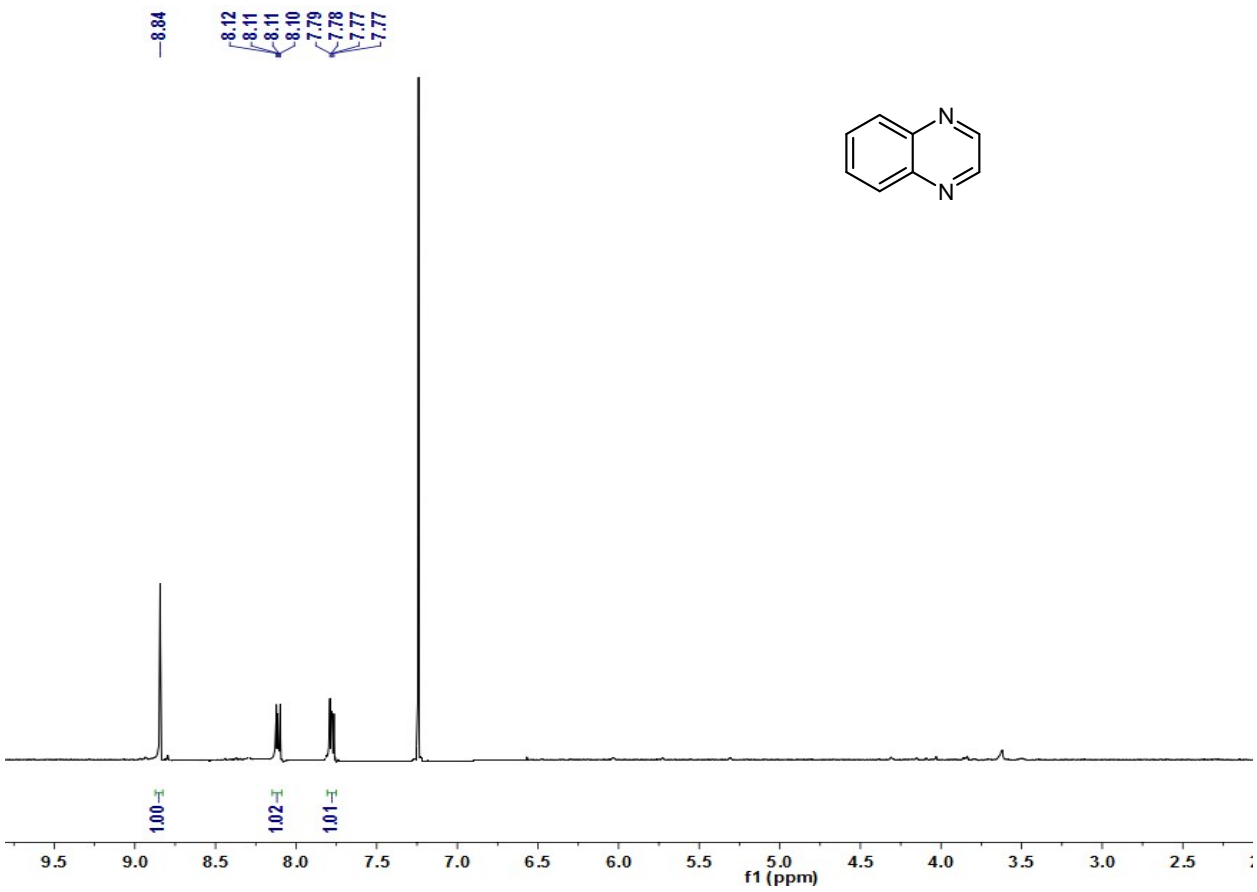
8.84
8.12
8.11
8.11
8.10
7.79
7.78
7.77
7.77
N
N
1.00
1.02
1.01
9.5
9.0
8.5
8.0
7.5
7.0
6.5
6.0
5.5
5.0
4.5
4.0
3.5
3.0
2.5
f1 (ppm)

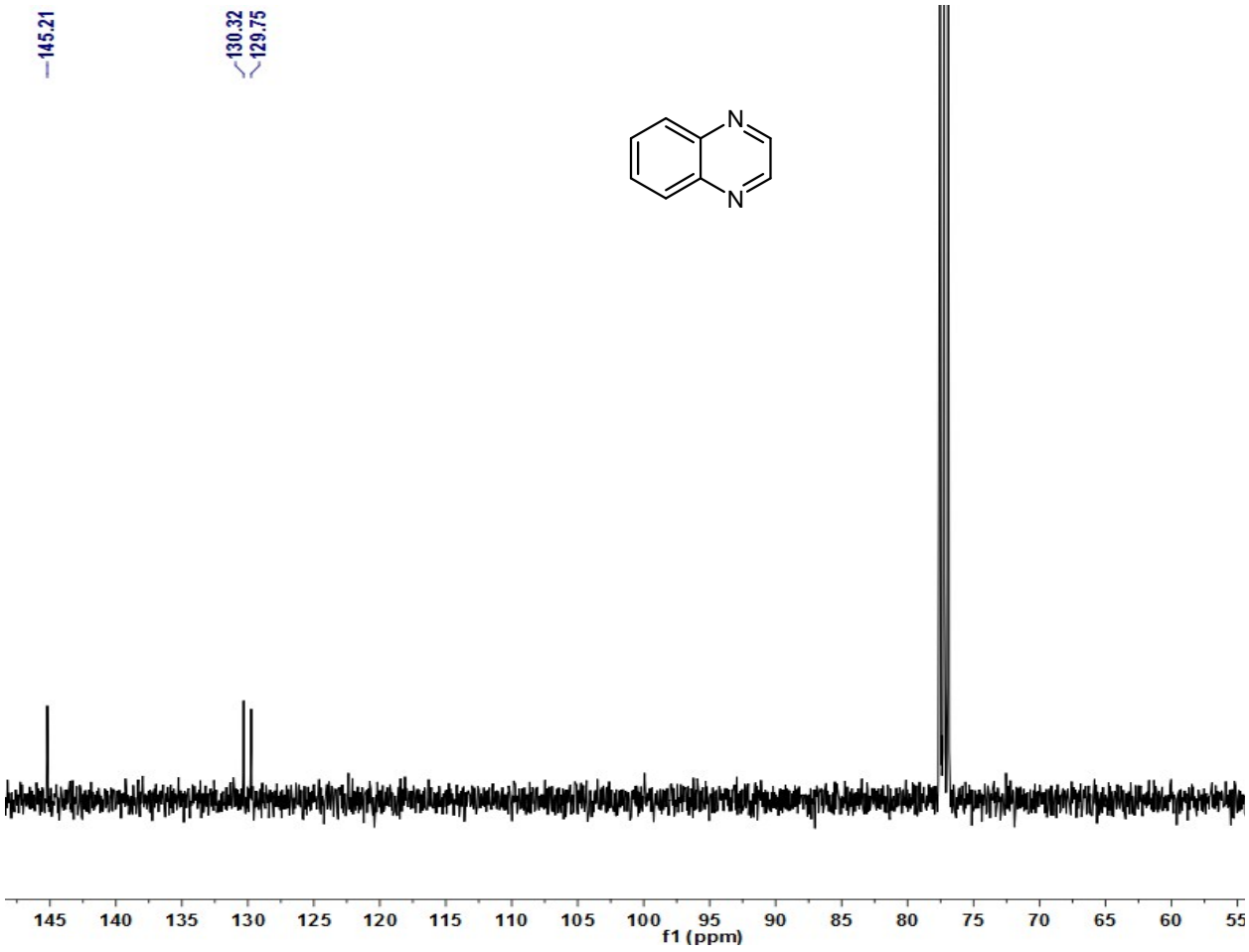
145.21
130.32
129.75
N
N
145
140
135
130
125
120
115
110
105
100
95
90
85
80
75
70
65
60
55
f1 (ppm)

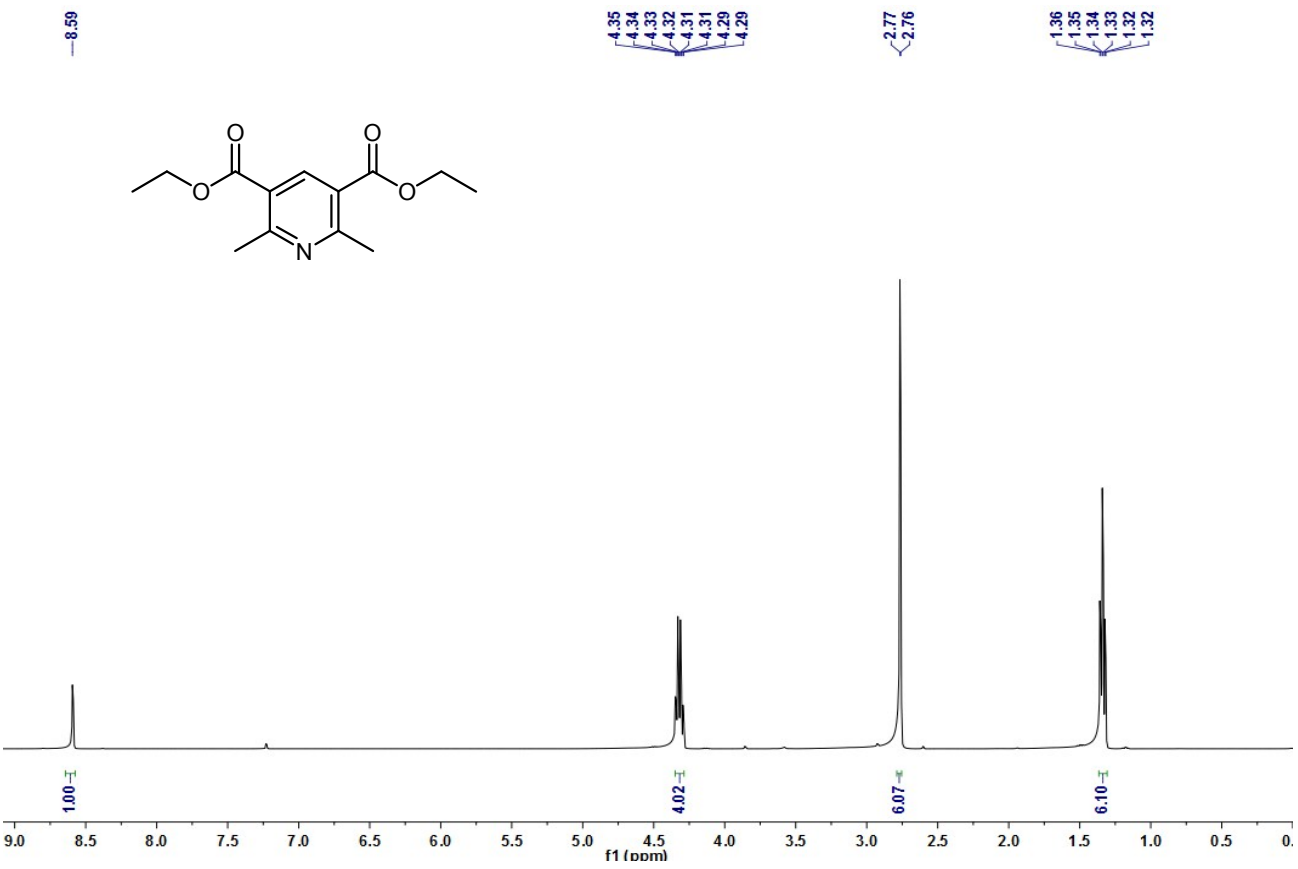
8.59
4.35
4.34
4.33
4.32
4.31
4.31
4.29
4.29
2.77
2.76
1.36
1.35
1.34
1.33
1.32
1.32
O
O
O
O
N
1.00
4.02
6.07
6.10
9.0
8.5
8.0
7.5
7.0
6.5
6.0
5.5
5.0
4.5
4.0
3.5
3.0
2.5
2.0
1.5
1.0
0.5
f1 (ppm)

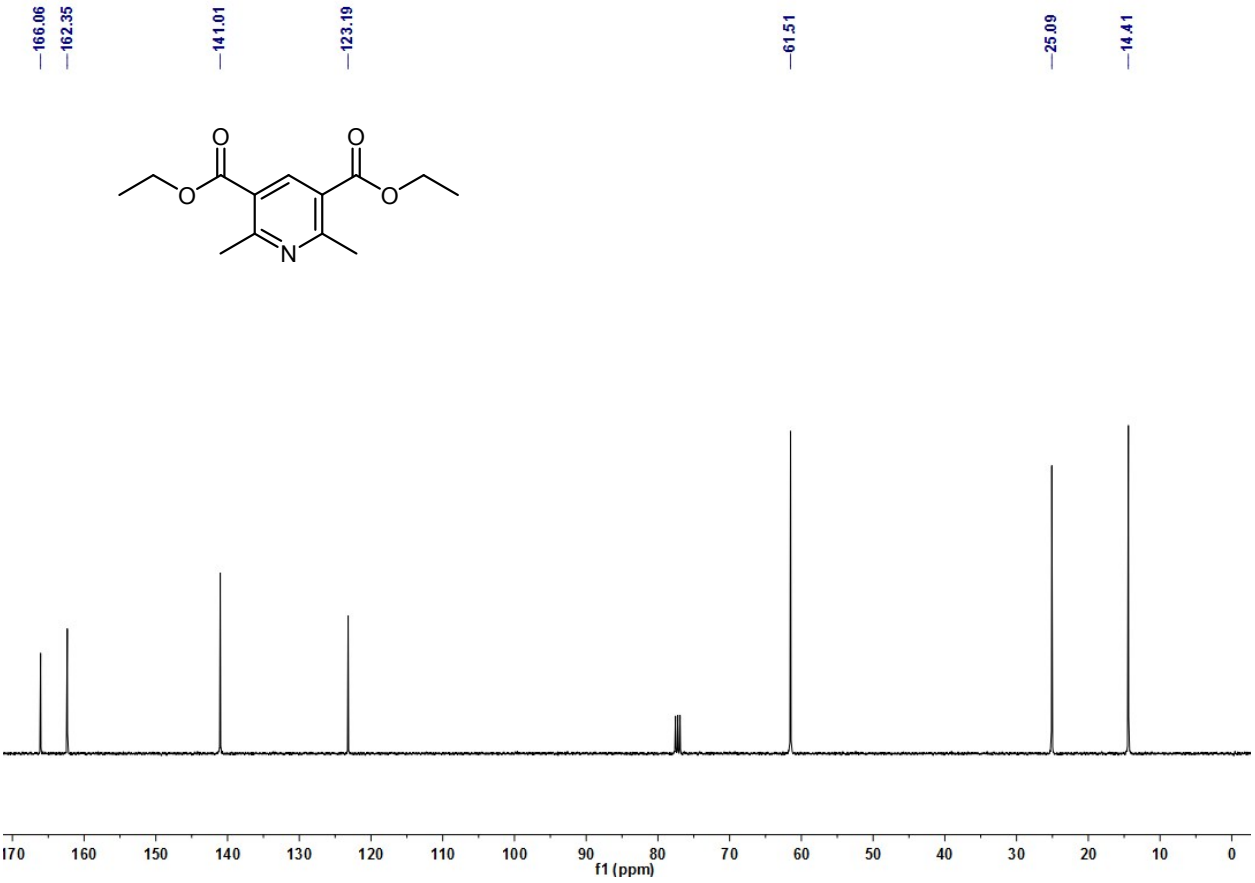

References

1. A. S. Poyraz, C.-H. Kuo, S. Biswas, C. K. King'ondu and S. L. Suib, *Nat. Commun.*, 2013, **4,** 2952.